ISSN 0023-1584, Kinetics and Catalysis, 2006, Vol. 47, No. 2, pp. 257–267. © MAIK "Nauka/Interperiodica" (Russia), 2006.

Chain "Stationary" Insertion Mechanism and Production of Isotactic Polypropylene with C_1 Symmetric Catalyst Systems[1]

A. Razavi[a], V. Bellia[a], D. Baekelmans[a], M. Slawinsky[a], S. Sirol[a], L. Peters[a], and Ulf Thewalt[b]

[a] *Centre de Recherche Du Groupe Total, Zone Industrielle C, B-7181 Seneffe (Feluy), Belgium*

[b] *Sektion für Roentgen und Elektronenbeugung, Universität Ulm, Germany*

e-mail: abbas.razavi@atofina.com

Received August 8, 2005

Abstract—In this contribution, the stereochemistry of propylene insertion/propagation reactions with a variety of C_1 symmetric metallocene catalysts, containing bridged cyclopentadienyl-fluorenyl ligand for the preparation of highly stereoregular polypropylene is presented. The impact of the distal substituent's size and composition and changes that the catalytic sites undergo upon such substitution is elaborated. A comprehensive mechanism is proposed to explain the resulting catalytic changes that bring about the irreversible C_s/C_1 site transformation and tactic behavior inversion. Furthermore the cyclopentadienyl's combined distal/proximal and fluorenyl's frontal substituent effects on molecular weight, regio-, and stereoregularity of the final polymers are discussed. Finally, stereoselectivities of C_2 and C_1 symmetric catalyst systems are compared. It is shown that current high performance C_1 symmetric catalyst systems with central site chirality can be isotactic selective as well or even better in certain aspects than the C_2 symmetric bridged bisindenyl-based metallocene catalysts.

DOI: 10.1134/S0023158406020169

INTRODUCTION

The pervasive commercial interest in metallocene-based polyolefins and their consequent large-scale production and applications in industrial facilities emanate from the capability of designing "perfect" metallocene-based catalytic systems. These catalysts permit the precise control over a polymer's degree of chemo-, regio-, and stereopurity; molecular weight; and weight distribution for accessing economically viable new or improved polymeric materials. Metallocene catalysts are nowadays used for the production of a variety of ethylene and propylene homo- and copolymers, as well as homo- and copolymerization of other olefins; the focus in this paper will be, however, on metallocene catalysts for the production of stereoregular polypropylene.

From different classes of metallocene catalysts capable of producing stereoregular polypropylene, those with bridged cyclopentadienyl-fluorenyl ligand are best suited as an ideal candidate for both academic investigation and industrial application. They distinguish themselves from conventional Ziegler–Natta catalysts and other classes of metallocene in providing a variety of polymers with unique and desirable properties by simple modification of their basic ligand skeleton. Their polymers differ, in many ways, from polymers produced with other metallocene-based catalysts, including those produced with C_2 symmetric bridged bicyclopentadienyl and bisindenyl counterparts. Their structural rigidity, chiral mode, degree, and facility of haptotropic isomerization are, inter alia, factors that determine physical, mechanical, and rheological features of their final polymers. In this contribution, we shall discuss these catalysts in a systematic way; however, we shall limit our discussion on C_s symmetric syndiotactic selective systems only to the basics since they have been largely covered in many recent articles. We commence the discussion by reiterating some important mechanistic elements of their stereochemistry that are essential for understanding the kinetic and mechanistic aspect of the C_1 symmetric catalyst systems.

[1] The text was submitted by the authors in English.

RESULTS AND DISCUSSION

Chain Migratory Insertion

The stereochemistry of propylene polymerization with C_s symmetric metallocenes, containing bridged cyclopentadienyl-fluorenyl ligand, has been thoroughly under investigation since their discovery in the late 1980s [1–6]. They have contributed a great deal to our basic understanding of olefin coordination polymerization. Figure 1 represents the X-ray structures of (η^5-C_5H_4-CMe_2-η^5-$C_{13}H_8$)MCl_2; M = Zr (**1**), Hf (**2**) [6]. **1** and **2** in combination with MAO were used to prepare the first highly crystalline syndiotactic polypropylene samples. The structure, catalytic properties, and the origin of the formation of syndiotactic chains with…*rrrrrrrrrmrrrrrrrrrrrrrrrmmrrrrrrr*… microtacticity with these catalytic systems have been discussed exhaustively in numerous publications [1–15, 31, 34, 35, 40, 51–53, 55–62].

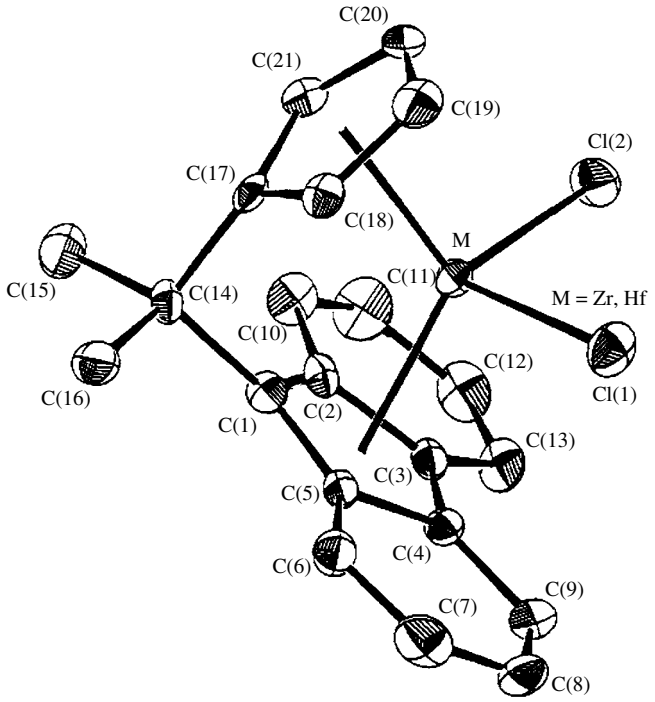

Fig. 1. Side view of the molecular structure of (η^5-C_5H_4-CMe_2-η^5-$C_{13}H_8$)MCl_2; M = Zr (**1**), Hf (**2**).

After activation with MAO or any alkylating and ionizing agents, **1** and **2** form chirotopic, cationic alkyl metallocenium species [8] that have the necessary vacant site and fragment orbitals for the coordination and activation of propylene monomers (Fig. 2). These cationic species are composed of equal numbers of *R* and *S* enantiomers with a preference for monomers' re or si faces. The chain migratory insertion mechanism transforms the *S* and *R* species into one another after each olefin insertion. The systematic transformation of the two antipodes into one another implies that the relative positions of two σ-bonded ligands, in the equatorial plane of the transition metal, are exchanged and monomers with alternative faces are coordinated and inserted, resulting in the formation of sequences of monomer units with alternating relative configuration, i.e., syndiotactic chains (Fig. 3).

Malfunctioning of the chain migratory insertion mechanism in this system due to lowering of the monomer concentration, increasing the polymerization temperature, and the use of polar solvents and/or coordinating counterions will trigger the so-called chain back migration or site epimerization mechanism (vide infra) and will result in the formation of occasional stereoerrors with two monomer units having the same relative configuration, the meso dyad m defects.

Figure 4 represents the transition state structure and mechanism of the ligand assisted re and si face selectivity process in syndiotactic selective systems. Figure 4 shows, in a schematic way, that the lowest energy pathway in the stereoselectivity process is induced via the unique steric arrangement of the chelating organic ligand that engulfs the resident transition metal. The steric interaction between the flat and spatially extended fluorenyl ligand forces the growing polymer chain to orient itself towards the free quadrants left or right of the unsubstituted cyclopentadienyl moiety of the ligand. The incoming monomer in turn—to avoid excessive steric exposure—coordinates to the metal in a manner that its methyl group is trans (or anti) positioned with respect to the growing polymer chain. In

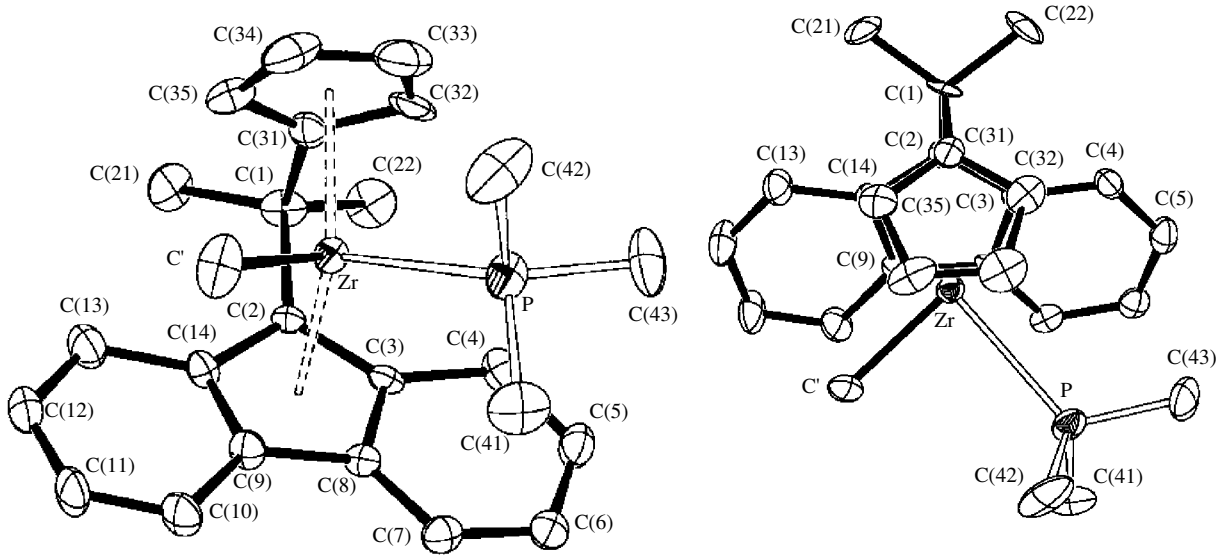

Fig. 2. Two views of the cation in the salt [(η^5-C_5H_4-CMe_2-η^5-$C_{13}H_8$)$ZrMe(PMe_3]^+[B(C_6F_5)_4]^-$. The [($\eta^5$-$C_5H_4$-$CMe_2$-$\eta^5$-$C_{13}H_8$)$ZrMe]^+$ cation is stabilized (right figure) with trimethylphosphine, which occupies the monomer coordination position [8].

this orientation, the coordinated monomer points with its methyl group "head down" into the free space in the central region of the fluorenyl ligand. The enantiomorphic site stereochemical control related errors occur whenever the aforesaid delicately balanced, nonbonded steric interaction is perturbed. In such a case, a monomer with the "wrong face" will be coordinated/inserted and a unit with inverted configuration is enchained. As a consequence, mm triad defects consisting of three monomer units with the same relative configuration are formed. The reverse face selectivity emanates from inherent steric and static structural factors and is independent of monomer concentration.

The "head-down" coordination mode of the monomer was determined after extensive molecular mechanics and force-field calculations performed by Corradini, Cavallo, and coworkers [16, 17]. Its correctness was confirmed repeatedly in recent years by more sophisticated molecular mechanics/quantum mechanics calculation. The model later underwent additional refinements and took its current form after experiments conducted by several groups [18–22] established α C–H agostic bond formation in the transition state (Fig. 4).

Reversible C_s/C_1 Site Transformation, Site Epimerization, Counterion Effect

Whereas understanding the origin of the formation of meso triad errors was straightforward and could easily be traced back to the enanionmorphic site control related error that was recognized decades ago in classical Ziegler–Natta systems, the reasons for the formation of meso dyads, m, were more complex and sometimes misleading [23–26].[1] It is related to a process called site epimerization according to which the catalyst site occasionally skips one olefin insertion as a result of occasional chain back migration.

The net effect of this skipped insertion is the enchainment of two consecutive monomers at the same enantiomorphic site and formation of meso dyad units with the same relative configurations.

This situation is visualized in the scheme shown in Fig. 5. Its origin can be traced back to the mechanism of chain back migration proposed by Cossee and Arlman in 1964 [27–29], to which it is conceptually very similar. According to these authors, the polymer chains connected to active $TiCl_5R$ sites, imbedded in the ionic

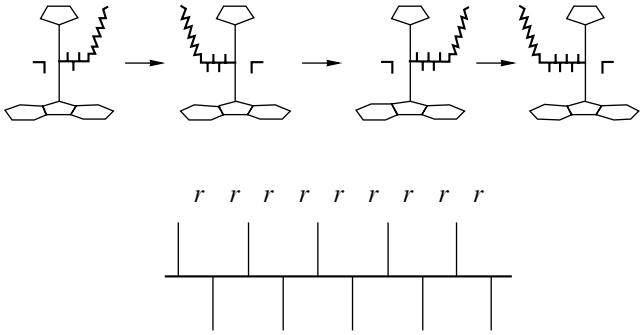

Fig. 3. Schematic representation of mechanism of syndiospecific polymerization (top). Fischer projection of a perfect syndiotactic chain (bottom).

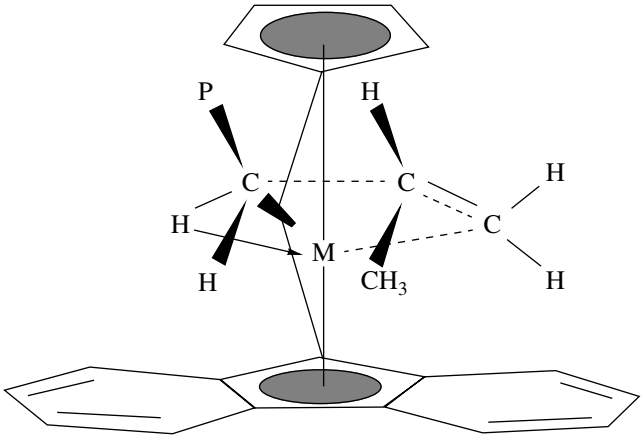

Fig. 4. Generally accepted transition state structure with polymer chain orientation with an (α-agostic H–Zr bond and trans (anti) monomer coordination mode.

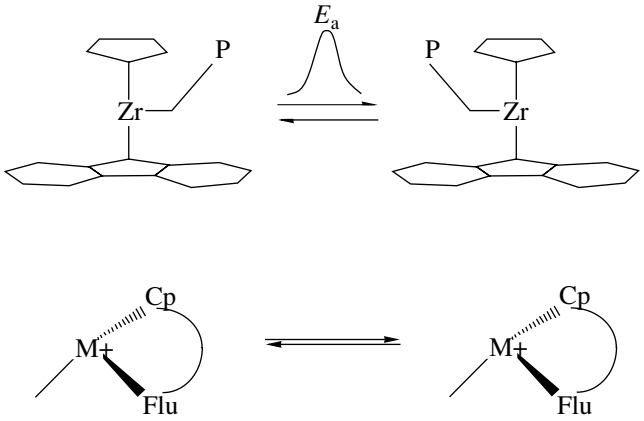

Fig. 5. Schematic representation of endothermic active site epimerization process (top). Out-of-plane orientation of the chain (bottom).

[1] The microstructure of syndiotactic polypropylene produced under a enantiomorphic site controlled mechanism is deceptively similar to syndiotactic polymers produced under the chain-end controlled mechanism when the fraction of site epimerization related meso dyad stereodefects is larger than meso triad, mm, defects related to reversed enatiofacial selectivity. Under these circumstances, the discrimination between the two mechanisms based on ^{13}C NMR spectroscopic configurational analysis could become problematic particularly when the resolution of the spectrum is low and peak overlapping complicates the integration [26]. References [23–25] are examples where the misinterpretation of ^{13}C NMR data has led to the wrong mechanism. The authors of [23] claim a chain-end controlled mechanism for the formation of syndiotactic polypropylene with a chiral catalyst at high temperature.

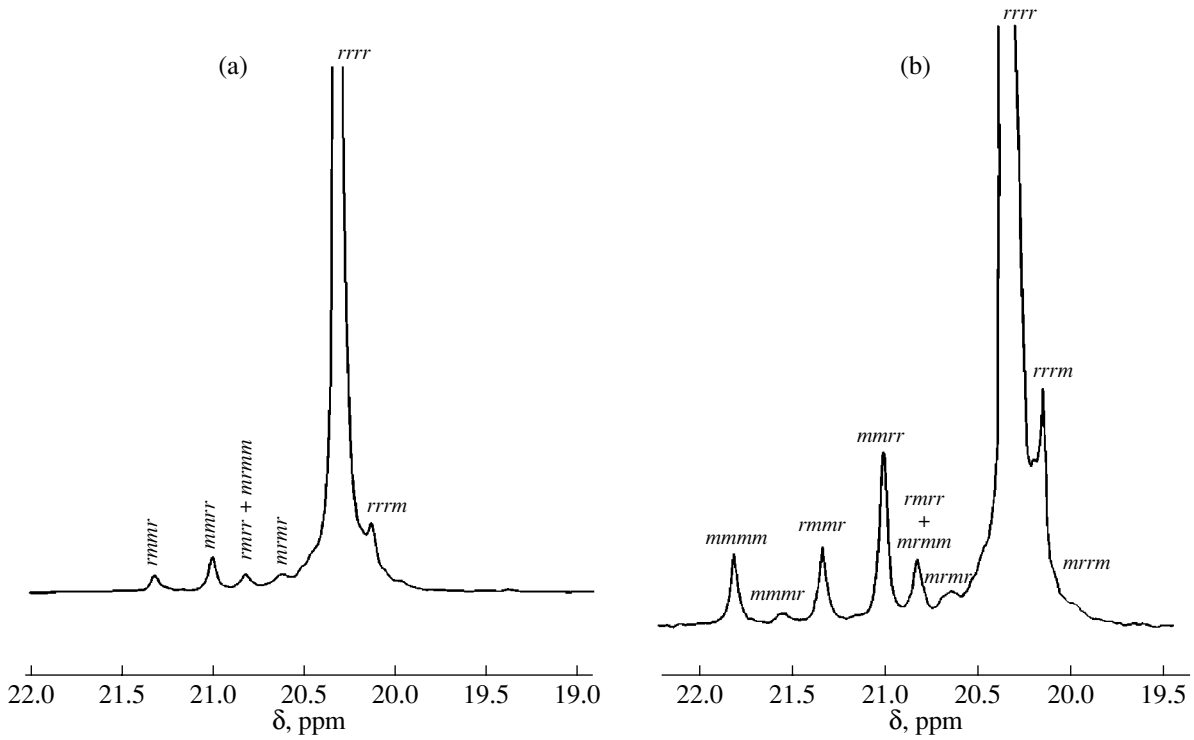

Fig. 6. ^{13}C NMR of syndiotactic polypropylene produced with (a) Zr- and (b) Hf-based catalysts.

lattice, undergo systematic back migration after each insertion owing to the changes in the relative ionicity of their immediate environments. In the case of metallocene catalysts, an increase in polymerization temperature, a decrease in monomer concentration, and the close proximity of the counterion can cause the site epimerization either by facilitating the chain back migration or by intermittent blockage of one of the coordination sites via a tight contact ion pairing.

We had suspected and suggested [6] this mechanism to be the cause of the formation of short isotactic blocks detected in the backbone of the predominantly syndiotactic polymer chains formed with **2**/MAO. Figure 6 represent the methyl region of the ^{13}C NMR spectra of syndiotactic polymers produced with **1** and **2**/MAO catalyst systems. In the ^{13}C NMR spectrum of syndiotactic polymer formed with **2**/MAO, a signal at 21.85 ppm indicates the presence of about 2% *mmmm* meso pentads. These isotactic pentads could have been formed only as a result of several consecutive insertions at the same enantiomorphic coordination site owing to tight ion pairing between the second coordination site and MAO anion [6].

Under these conditions, the contact ion-paired complex becomes an active site with temporary coordination site inequivalence and undergoes a reversible C_s/pseudo-C_1 site symmetry transformation. Consequently, several insertions at the same enantiomorphic coordination site may occur, leading to the formation of a short isotactic sequence within the predominantly syndiotactic chain. The lower activity of the catalyst formed with **2**/MAO and higher molecular weights of the polymers could also be related to this tight contact ion pairing. The close proximity of the anion partially "quenches" the electrophilicity of the Hf cation, lowers the Hf–C bond polarization, and decreases the propagation rate by increasing the insertion activation energy barrier. Lower Lewis acidity of the cation in contact with the counterion, on the other hand, lowers its propensity for β-hydride abstraction and leads to an increase in molecular weight of the polymers. There is also a steric reason. The anion, in the contact ion-paired complex, interacts sterically with the polymer chain and prevents its proper approach for a β-agostic interaction. The observation made by Rieger [30] that "noncoordinating" anions bearing activators such as trityltetrakis(pentafluorophenyl)borate provide substantially higher activities for hafnocene-based catalysts is well in consonance with this argument. These observations add to the growing pool of evidence that the presence of an anion in the coordination sphere of the transition metal can alter the behavior of the complex.

The inequivalence of coordination sites caused by the counterion, via occasional contact ion pairing, can be tuned in a more controlled and systematic way by the introduction of distal substituents into cycolpentadienyl moiety of the ligand. β-Substituents with gradually increasing steric bulk and repulsive nonbonded interaction with the migrating polymer chain will enhance the site epimerization processes. The initially

Table 1. Polymerization results and polymer analyses for the **3**/MAO catalyst system

T, °C	M_w, kD	Stereoregularity *mmmm*, %	Regiodefects, %	Melting point, °C
40	75000	78.02	0.4	129
60	62000	77.47	0.4	127
80	48000	75.80	0.4	127

Note: kD—kiloDalton.

marginal site epimerization rate increases with increasing size of the substituent and enters into serious competition with the olefin insertion rate to finally become dominant at a critical substituent size. In parallel, the frequency and lengths of the isotactic sequences, meso dyads, increase in the predominantly syndiotactic polymer chains [31]. Distal substituents such as phenyl, methyl, ethyl, isopropyl, tertiaryl butyl, and trimethylsilyl have been implanted in the cyclopentadienyl's distal position of **1**, and polymers with hemi-isotactic, partially isotactic and polymers with mixed tacticity [32–39] have been obtained with resulting catalysts. The most remarkable results were, however, produced with a tertiary butyl (and trimethylsilyl) group as a substituent. In these instance(s), as we shall see below, the site epimerization rate is accelerated to the extent that the chain migratory insertion rate becomes marginal and the tactic behavior of the catalyst is completely reversed. An originally syndiospecific catalyst became isotactic selective, via the addition of a "simple" substituent.

Distal Substituent, Irreversible Site Transformation, Chain "Stationary" Insertion Mechanism

The crystal structure and polymerization behavior of the (η^5-3-*t*-Bu-C_5H_3-CMe_2-η^5-$C_{13}H_8$)$ZrCl_2$ (**3**) have been discussed elsewhere [40–42]. Table 1 summarizes the polymerization results and some polymer properties obtained with **3**/MAO. The formation of the isotactic polymers with this catalyst system was explained according to a mechanism that we described as chain "stationary" insertion mechanism. According to this mechanism, the quasi-complete blockage of one of the catalyst's coordination positions, by a bulky distal substituent, creates a symmetry-breaking site differentiation. The bulk of the substituent forces the coordinating monomer and polymer chain to selectively reside at one coordination site or the other. This leads to the domination of the site epimerization process and chain stationary insertion. Under these conditions, from the incoming monomer's perspective, the growing polymer chain appears "stationary" by attacking predominantly from the same coordination position [40–42]. This mechanism is depicted in Fig. 7. The *t*-butyl group's role is instrumental in creating the condition for the symmetry-breaking site differentiation caused by permanent C_s/C_1 site transformation.

The chain "stationary" insertion hypothesis is supported by the selective absence of *mmrm* and *rmrm* steric pentad distribution signals in the ^{13}C NMR spectra of the isotactic polymers produced with **3**/MAO [40–42]. The absence of these pentads reflects the low probability of occurrence of two consecutive stereoerrors at the same coordination position or the low probability for the chain to reside at the more crowded coordination position. It provides the key clue for the accelerated site epimerization processes being the dominating mechanism involved in polymerization with this catalyst system. Additionally, the polymerization temperature enhancing effect [43–45] on the isospecificity of **3**/MAO (vide infra)—in drastic contrast to Brintzinger type C_2 symmetric isoselective systems [46, 47]—can be seen as a further clue for the operating epimerization processes. Finally, molecular mechanics analysis and energy calculations performed by Guerra et al. on similar systems are also supportive of a site epimerization controlled mechanism for this catalyst [48–50].

Combined Proximal/Distal Substituent Effect

A cursory glance at the data presented in Table 1 reveals that, despite very interesting academic aspects of this catalyst system, the resulting low-molecular-weight isotactic polymers are of little practical interest. Polymer stereoregularities are relatively low and the isotactic chains are plagued with nonnegligible amounts (0.4%) of regiodefects. Since a further increase in the steric bulk of the substituent, from *t*-butyl to trimethylsilyl, did not bring about the expected and desired improvements and resulted in a different polymer as reported [51–54], a different path was chosen to reach this goal. We decided this time to

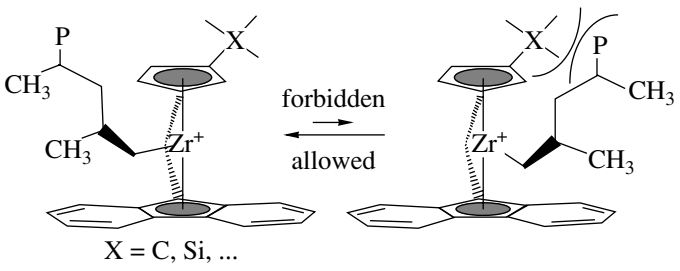

Fig. 7. Nonbonded steric repulsion between polymer chain and β-substituent promoting site epimerization.

Table 2. Polymerization results and polymer analyses with **4**/MAO system

T, °C	M_w, kD	Stereoregularity *mmmm*, %	Regiodefects, %	Melting point, °C
40	580000	79.12	nd	132
60	402000	86.3	nd	144
80	213000	83.6	nd	142

Note: kD—kiloDalton, nd—not detected.

modify the structure of **3** by implanting a second, smaller, substituent in its proximal position and prepared the metallocene dichloride (η^5-3-*t*-Bu-5-Me-C_5H_2-CMe_2-η^5-$C_{13}H_8$)$ZrCl_2$ (**4**) [55–58]. The MAO activated complex **4** is a very effective catalyst for isospecific polymerization of propylene to polypropylene. Table 2 presents polymerization results and analyses of the polymers produced in liquid propylene at different temperatures with the **4**/MAO catalyst system.

Close inspection of the polymerization data given in Table 2 indicates that the introduction of *trans*-proximal methyl substituent in this molecule brings about substantial improvements in almost every aspect of the catalytic performance. The molecular weights of the polymers produced with the **4**/MAO catalyst system are substantially higher than those reported for the **3**/MAO counterpart. The isotactic polymer chains are perfectly regioregular and practically devoid of any 2–1 or 1–3 regiodefects. Most importantly, the stereoregularities (*mmmm* %) of the polymer chains produced with the **4**/MAO catalyst system are, by about 10%, substantially higher than the stereoregularities that have been recorded for the polymers produced with the **3**/MAO catalyst. As a consequence, the melting points of the corresponding isotactic polymers reach values over 140°C, even for the polymers that were formed at 80°C. Noteworthy is the relationship of polymer stereoregularities with the polymerization temperature. An increase in the polymerization temperature from 40 to 60°C leads to an improvement in catalyst stereoselectivity and polymer stereoregularity owing to the accelerated site epimerization; however, a further increase in polymerization temperature, from 60 to 80°C, causes a slight decrease in stereoselectivity.

An apparent drastic suppression of β-hydride elimination and 2–1 insertion related processes must have led to the substantial increase in molecular weights and regio- and overall stereoregularity of the polymers. Figure 8 represents two perspective views of molecular structure of **4** determined by single-crystal X-ray diffraction analysis. These views illustrate pictorially the position of the proximal methyl group (designated by C41), in the upper back section of the molecule. This methyl substituent is positioned in such a way that it would necessarily interfere with the methyl group of propylene monomer in a 2–1 coordinated mode (should the monomer choose this coordination position). In this position, it also interferes sterically with the cyclic tran-

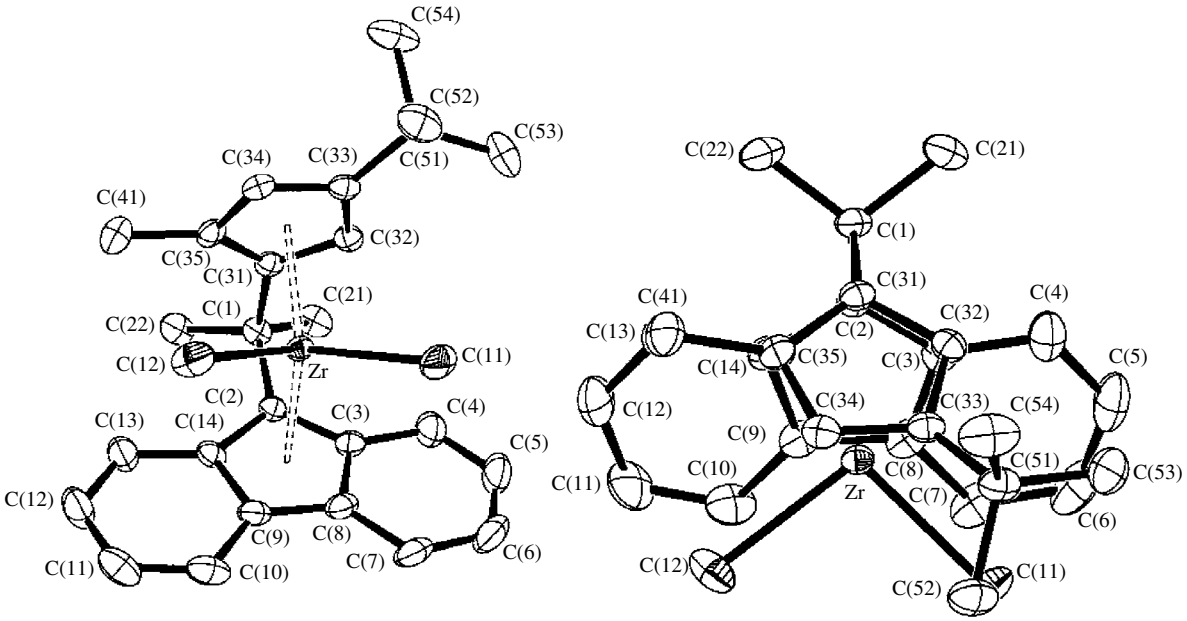

Fig. 8. Two views of the molecular structure of η^5-3-*t*-Bu-5-Me-C_5H_2-CMe_2-η^5-$C_{13}H_8$)$ZrCl_2$ (**4**).

sition state structure—a prerequisite for any kind of β-hydride transfer—involving the transition metal, polymer chain, and the monomer. Figure 9 illustrates this process schematically in a pictorial way. In a front-side propylene coordination mode, the transition state metalla-cyclohexane can be formed, which assists the β-hydrogen transfer to the monomer in **3**/MAO, leading to low-molecular-weight isotactic polypropylene. The proximal methyl substituent in **4** interferes with the formation of this transition state structure and prevents its formation. This explains the high molecular weight of the polymers formed with the **4**/MAO catalyst system.

Whereas the rationalization of the β-hydride elimination suppression seems straightforward and is in line with the observation that has been made for bridged substituted bicyclopentadienyl- and bisindenyl-based metallocene catalyst systems [46, 47], the mechanism of the suppression of 2–1 insertion and improved enantioselectivity needs further elaboration.

Considering the fact that, for C_1 symmetric systems (the type discussed here), the probability of the monomer coordination/insertion at the less crowded site is low, the quasi-complete suppression of the regiodefects in isotactic polymers formed with the **4**/MAO catalyst system needs further clarifications. It would mean that (1) in the **3**/MAO catalyst system, the chain occasionally moves to the crowded coordination position; (2) the monomer coordinating the less crowded position is less face selective; and (3) when the chain is placed at the crowded coordination position, in the absence of any other steric factors, it forces most of the reverse face coordinated propylene to rotate, adopt a 2–1 coordination mode, and undergo a regioirregular insertion that could be followed more easily by a β-hydride elimination and chain termination. The *trans*-proximal methyl substituent in the **4**/MAO catalyst system, by its nonbonded steric interaction, apparently counterbalances the steric force of the polymer chain on the propylene monomer and prevents this rotation and therefore does not permit a 2–1 coordination/insertion. Furthermore, the overall higher enantioselectivity of **4**/MAO compared to the **3**/MAO catalyst system could indicate that most reverse face coordinated monomers, exposed simultaneously to two different steric forces, dissociate from the catalysts site in the **4**/MAO system and have less chance to give rise to a nonstereoselective insertion.

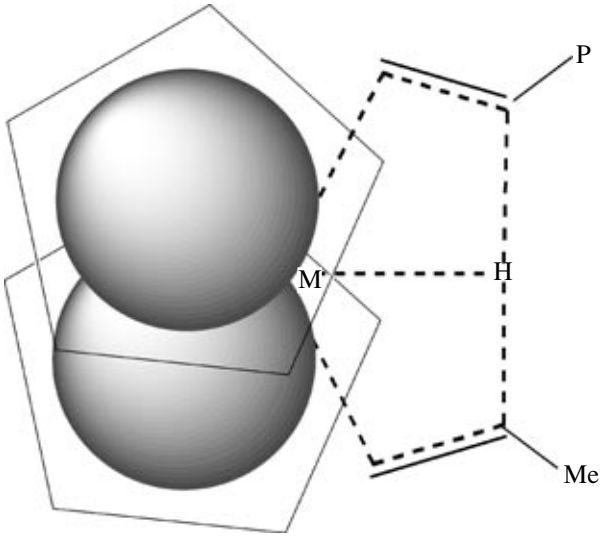

Fig. 9. A front-side propylene coordination mode and the transition state structure for β-hydrogen transfer in **3**. Proximal methyl substituent in **4** interferes with the formation of this transition structure.

Perfect Chain Stationary Insertion, Perfect Isoselectivity

While discussing the C_s symmetric syndiotactic selective systems, we have shown in previous publications [13, 14–62] that the 3,6-bulky substitution in the frontal positions of the fluorenyl moiety of the ligand is very beneficial for improving the catalyst's stereoselectivity. The frontal bulky substituents interact with the counterions and prevent the formation of tight contact ion pairing. Additionally, because of their spatial expansion, they interact strongly, in a nonbonded fashion, with the growing polymer chain and enhance its preferred orientation into the empty quadrant(s) next to cyclopentadienyl moiety of the ligand. As a result, a tighter chiral pocket is formed in which the corresponding re and si monomer faces would fit better and coordinate/insert with increased selectivity. The same argument should in principle hold for C_1 symmetric, isotactic selective catalyst systems, albeit only operational for one of the catalyst's coordination sites. To prove this hypothesis, we prepared a new metallocene molecule. Figure 10 represents the front and top views of the molecular structure of the metallocene, (η^5-3-*t*-Bu-2-Me-C_5H_2-CMe_2-η^5-3,6-di-*t*-Bu-$C_{13}H_6$)$ZrCl_2$ (**5**) deter-

Table 3. Polymerization results and polymer properties of isotactic polypropylene formed with **5**/MAO catalysts system

T, °C	M_w, kD	Stereoregularity *mmmm*, %	Regiodefects, %	Melting point, °C
40	1.363	97.30	nd	157.2
60	515.4	98.07	nd	162.2
80	215.0	94.18	nd	155.7

Note: kD—kiloDalton, nd—not detected.

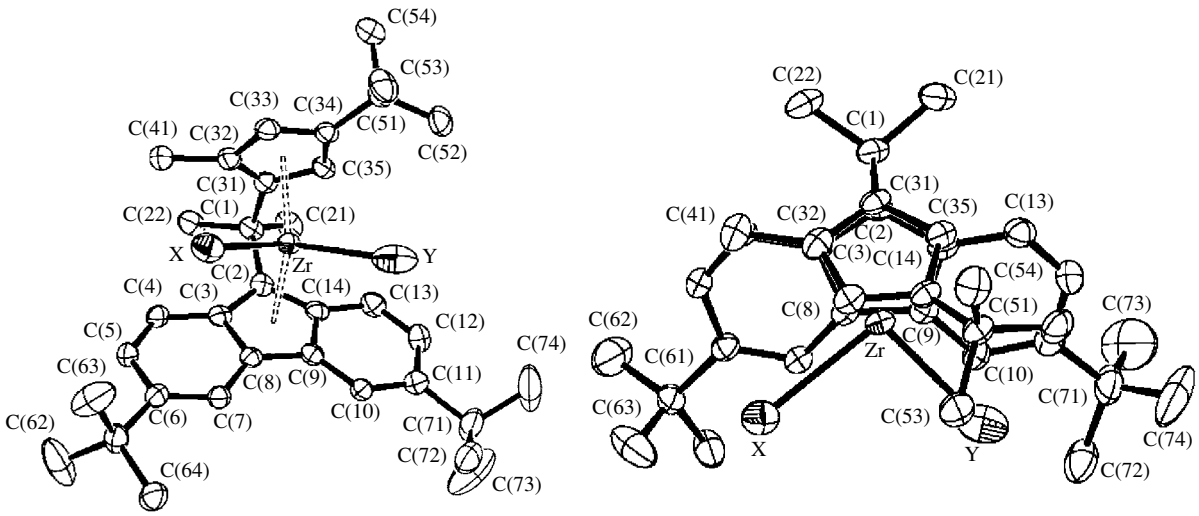

Fig. 10. Two views of the molecular structure of η^5-3-*t*-Bu-5-Me-C_5H_2-CMe_2-η^5-3,6-di-*t*-Bu-$C_{13}H_6$)$ZrCl_2$ (**5**).

mined by single crystal X-ray diffraction methods. Table 3 summarizes the polymerization results and polymer properties of isotactic polypropylene formed with the **5**/MAO catalyst system at different polymerization temperatures.

The data in Table 3 indicate that, as expected, the isotactic polymers produced with the **5**/MAO catalyst system exhibit both higher molecular weights and substantially higher stereoregularities (cf. *mmmm* % and polymer melting points) compared to the corresponding polymers produced with **4**/MAO. Similar to polymer formed with **4**/MAO, no regiodefects have been detected in ^{13}C NMR spectra of the isotactic polymers that have been produced with **5**/MAO. The data in Table 3 also reveal a similar correlation between polymerization temperature and the catalyst's stereoselectivity to that observed with catalyst system **4**/MAO. By increasing the polymerization temperature from 40 to 60°C, catalysts' stereoselectivity is increased, as is apparent by the polymers' melting points and tacticity indexes (*mmmm* %). However, when the temperature is further raised from 60 to 80°C, the beneficial effect of site epimerization rate increase on stereoselectivity is overcompensated by an increasing number of reverse-face selective insertions and formation of a larger number of meso triad, mm, stereoerrors.

With **5**/MAO, we have for the first time a metallocene catalyst at hand that produces, at relatively high polymerization temperatures, isotactic polypropylene polymers with high molecular weights and melting points, rivaling isotactic polymers that are produced commercially with high performance isotactic selective Ziegler–Natta catalyst systems with an additional advantage of having narrow molecular weight distribution and no atactic fraction. The quasi-perfect stereoselectivity of this catalyst is an indication of the absolute prevalence of site epimerization and the chain stationary insertion mechanism over the chain migration insertion mechanism. In conclusion, the chain "stationary" insertion mechanism that we introduced a decade ago [40, 41] as the working hypothesis to explain the formation of isotactic polypropylene with **3**/MAO seems vindicated. This hypothesis, which did not seem obvious at the time, is a logical extension and generalization of the site epimerization mechanism. It helped us to rationalize the polymerization behavior of C_1 symmetric metallocene catalysts and elucidate the microstructure of their isotactic polymers. Additionally, it also led to the development of new C_1 symmetric metallocene catalyst systems such as **4**/MAO with much better catalytic performance. Finally, the combination of strategies developed for improving the catalytic performance of C_s (fluorenyl's frontal substation effects) and those adopted for improving the C_1 symmetric catalyst systems led to the development of the high-performance isotactic selective **5**/MAO catalyst system. The polymerization processes leading to the formation of isotactic polymer with **5**/MAO, conversely, confirm the absolute dominance of site epimerization over chain migration in these systems. Only the perfect functioning of the chain "stationary" insertion mechanism could give rise to isotactic polymer chains with almost perfect isotacticity. Figure 11 illustrates pictorially the prohibitively crowded coordination site, with two *t*-butyl groups above and below it. Both for steric and entropic reasons, this coordination position cannot accommodate the growing polymer chain. Under these conditions, the chain must reside at the sterically less crowded site and will have to return to this coordination site after each insertion.

C_1 Symmetry vs. C_2 Symmetry

Before ending this discussion, we should emphasize a few interesting and practical aspects of isotactic spe-

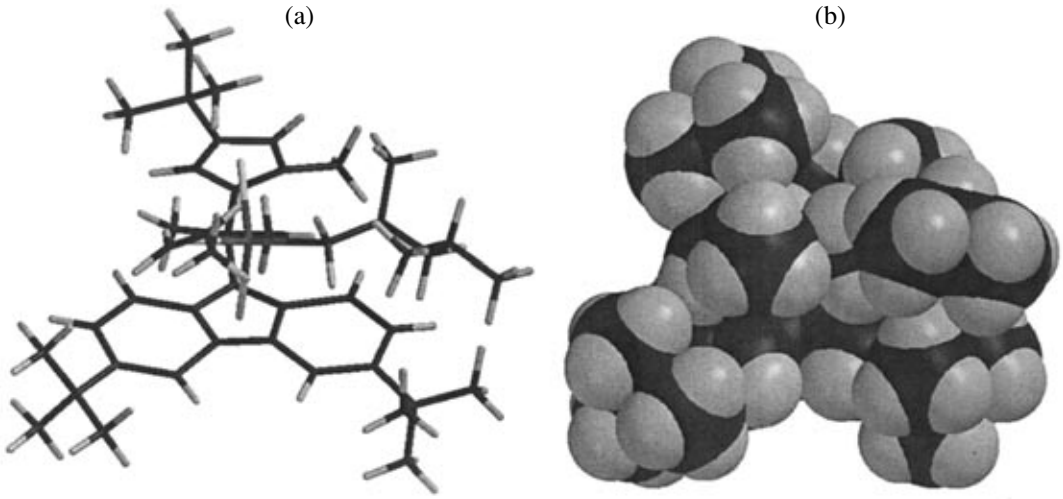

Fig. 11. Pictorial illustration of the crowded site with a coordinated propylene and the crowded coordination site with two *t*-butyl groups above and below it (a). Space filling model representation (b).

cific C_1 symmetric catalysts in comparison with their C_2 symmetric counterparts. The C_1 symmetric metallocene molecules do not undergo photo- or heat-induced isomerization during activation/heterogenization processes, nor is any meso stereoisomer formed during their synthesis. The meso stereoisomer is difficult to separate and often prone to formation of an atactic fraction mixed with isotactic polypropylene. Their stereoselectivities do not suffer by increasing polymerization temperatures; and in some C_1 symmetric systems (vide supra), they are even boosted. The trans-disubstituted C_1 symmetric system are very regioselective and maintain this property upon activation/heterogenization. This is again a major difference from C_2 symmetric, bridged bis-indenyl catalyst systems, where the resulting polymer can have up to 1% regiodefect. The trans-substituted C_1 symmetric systems are very regioselective [59–62] and maintain this property upon activation/heterogenization.

CONCLUDING REMARKS

To arrive at such a degree of catalyst performance perfection, gradual improvement of our understanding of underlying synthetic methods, polymerization processes, polymer analyses, and mechanistic aspects of polymerization were needed. Major advances in synthetic skills for preparation and isolation of sophisticated ligands and metallocene precatalyst components, precise control of polymerization conditions, and better resolution and interpretation of polymer analytical data, particularly ^{13}C NMR spectral data, were essential. Prior and parallel to the systematic application of site-selective substitution, it was also necessary to overcome many mechanistic challenges. The emergence of a wealth of computational publications covering theoretical aspects of the different stages of polymerization using powerful computers to perform ever more sophisticated MM/QM calculations [63–67] has helped to fine-tune our understanding of the different steps involved in polymerization.

The initial ideas and models based on which perfect bilateral symmetry (C_s symmetry) and enantiotopic coordination positions were considered as central dogmas for the syndiospecificity process were modified and gave room to models that are less focused on overall symmetry. They put more emphasis on flexible geometry of an active site [68–75] and dynamic behavior of a polymer chain (chain migration, back migration) and energetics involved in enantiodifferentiating processes. It is now evident that the static picture of a pseudotetrahedral geometry (Fig. 12 left), which was assumed for the tetra-coordinated transition metal alkyl olefin complex in the transition state, could not be further extended to the step just after insertion. At this stage, the tetracoordinated structure collapses owing to the disappearance of a ligand, the coordinated monomer, leaving behind a tricoordinated species in which the repulsive forces acting upon the bonding and nonbonding electron pairs are different and require a new geometry. The most logical structure that can be sug-

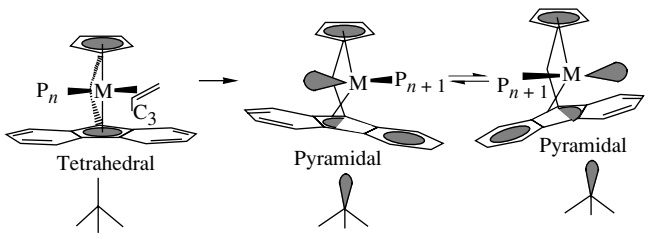

Fig. 12. Geometry variation during coordination and insertion steps and site epimerization.

gested for this step would obviously be a pyramidal [76] one capable of epimerizing (Fig. 12 right).

This change in geometry, operating on all types of metallocene-based catalyst systems, is more significant for the syndiospecific case where dynamic processes such as chain migration and more importantly site epimerization are more vital for its existence than for the isoselective systems.

The interaction with counterion, initially considered as very trivial, seems to gain more and more importance. A growing wealth of data indicate that including the anion in the coordination sphere of the transition metal can alter the behavior of the catalytic complex. The preference of these contact ion pairs for chain conformers without β-agostic interactions can be rationalized by electronic and steric factors. The electron deficiency of the metal cation is partly alleviated by coordination with the anion, making stabilization by agostic interaction less important. Thus, in addition to impacting the activity, the chain migratory insertion, and site epimerization processes, the counterion could modify the reaction paths of the elementary reactions and their activation energy barriers and thus change the whole course of stereoselection and chain formation processes [77–84].

REFERENCES

1. Ewen, J.A., Jones, L.R., Razavi, A., and Ferrara, J.J., *J. Am. Chem. Soc.*, 1988, vol. 110, p. 6255.
2. US Patent 5334677.
3. US Patent 5476914.
4. US Patent 6184326A.
5. US Patent 4892851.
6. Razavi, A. and Ferrara, J.J., *J. Organomet. Chem.*, 1992, vol. 435, p. 299.
7. Razavi, A. and Atwood, J.L., *J. Organomet. Chem.*, 1993, vol. 459, p. 117.
8. Razavi, A. and Thewalt, U., *J. Organomet. Chem.*, 1993, vol. 445, p. 111.
9. Razavi, A., Baekelmans, D., Bellia, V., de Brauwer, Y., Hortmann, K., Lambrecht, M., Miserque, O., Peters, L., Slawinsky, M., and van Belle, S., *Progress, Development of Catalytic Olefin Polymerization*, Sano, T., Uozumi, T., Nakatani, H., and Terano, M., Eds., Tokyo: Technology and Education, 2000, p. 176.
10. Razavi, A., *C. R. Acad. Sci., Ser. IIc*, 2000, vol. 3, p. 615.
11. Razavi, A., Hortmann, K., and Bellia, V., *Synthetic Methods of Organometallic and Inorganic Chemistry*, Herrman, W.A., Ed., Stuttgart: Thieme, 2002, vol. 10, p. 185.
12. Razavi, A., *C. R. Acad. Sci., Ser. IIc*, 2000, vol. 3, p. 615.
13. Razavi, A., Bellia, V., Debrauwer, Y., Hortmann, K., Peters, L., Sirole, S., Belle, S.V., Marin, V., and Lopez, M., *J. Organomet. Chem.*, 2003, vol. 684, p. 206.
14. Razavi, A., Bellia, V., Debrauwer, Y., Hortmann, K., Peters, L., Sirole, S., and Belle, S.V., *Macromol. Symp.*, 2004, vol. 213, p. 157.
15. Razavi, A., Bellia, V., Debrauwer, Y., Hortmann, K., Peters, L., Sirole, S., Belle, S.V., and Thewalt, U., *Macromol. Chem. Phys.*, 2004, vol. 205, p. 347.
16. Cavallo, L., Guerra, G., Vacatello, M., and Corradini, P., *Macromolecules,* 1991, vol. 24, p. 1784.
17. Guerra, G., Cavallo, L., Moscardi, L., Vacatello, M., and Corradini, P., *Macromolecules,* 1996, vol. 29, p. 8434.
18. Piers, W.E. and Bercaw, J.E., *J. Am. Chem. Soc.*, 1990, vol. 112, p. 9406.
19. Brintzinger, H.H. and Krauledat, H., *Angew. Chem., Int. Ed. Engl.*, 1990, vol. 29, p. 1412.
20. Brintzinger, H.H. and Leclerc, M.L., *J. Am. Chem. Soc.*, 1995, vol. 117, p. 1651.
21. Burger, B.J., Cotter, W.D., Coughlin, E.B., Chascon, S.T., Hajela, S., Herzog, T.A., Koehn, R.O., Mitchell, J.P., Piers, W.E., Shapiro, P.J., and Bercaw, J.E., *Ziegler Catalysts,* Fink, G., Muelhaupt, R.H., and Brintzinger, H.H., Eds., Berlin: Springer, 1995.
22. Grubbs, R.H. and Goates, G.W., *Acc. Chem. Res.*, 1996, vol. 29, p. 85.
23. Yu, Z. and Chien, J.C.W., *J. Polym. Sci., Part A: Polym. Chem.*, 1995, vol. 33, p. 125.
24. Hagihara, H., Shiono, T., and Ikeda, T., *Macromolecules,* 1997, vol. 30, p. 4783.
25. Hagihara, H., Shiono, T., and Ikeda, T., *Macromolecules,* 1998, vol. 31, p. 3184.
26. Busico, V., Cipullo, R., Cutillo, F., Talarico, G., and Razavi, A., *Macromol. Chem. Phys.*, 2003, vol. 204, p. 1269.
27. Cossee, P., *J. Catal.,* 1964, vol. 3, p. 99.
28. Arlman, E.J., *J. Catal.,* 1964, vol. 3, p. 89.
29. Arlman, E.J. and Cossee, P., *J. Catal.,* 1964, vol. 3, p. 99.
30. Rieger, B. and Troll, C., *Macromolecules,* 2002, vol. 35, p. 5742.
31. Razavi, A., Peters, L., Nafpliotis, L., Vereecke, D., and Den Daw, K., *Macromol. Symp.,* 1995, vol. 89, p. 345.
32. Farina, M., Silvestro, G., and Sozzani, P., *Macromolecules,* 1982, vol. 15, p. 1452.
33. Farina, M., Silvestro, G., and Sozzani, P., *Macromolecules,* 1985, vol. 18, p. 923.
34. Razavi, A. and Atwood, J.L., *J. organomet. Chem.*, 1995, vol. 497, p. 105.
35. Razavi, A, Vereecke, D, Peters, L, Den Dauw, K., Nafpliotis, L., and Atwood, J.L., *Ziegler Catalysts: Proc. Int. Symp. on Recent Scientific Innovations and Technological Improvements*, Fink, G., Muelhaupt, R., and Brintzinger, H.H., Eds., Berlin: Springer, 1995.
36. Herfert, N. and Fink, G., *Makromol. Chem., Macromol. Symp.*, 1993, vol. 66, p. 157.
37. Angermund, K., Fink, G., Jensen, V.R., and Kleinschidt, R., *Macromol. Rapid Commun.*, 2000, vol. 21, p. 91.
38. Ewen, J.A., Elder, M., Jones, L.R., Haspeslagh, L., Atwood, J.L., Bott, J.L., and Robinson, K., *Makromol. Chem., Macromol. Symp.*, 1991, vol. 48/49, p. 253.
39. Eur. Pat. Appl. EP 1095081.
40. Razavi, A. and Atwood, J.L., *J. Organomet. Chem.*, 1996, vol. 520, p. 115.
41. Razavi, A., Peters, L., and Nafpliotis, L., *J. Mol. Catal.*, 1997, vol. A, p. 129.

42. Busico, V., Cipullo, R., and Talarico, G., *Macromolecules,* 1997, vol. 30, p. 4787.
43. Razavi, A., Vereecke, D., Peters, L., Den Daw, K., Nafpliotis, L., and Atwood, J.L., *Ziegler Catalysts,* Fink, G., Muelhaupt, R., and Brintzinger, H.H., Eds., Berlin: Springer, 1993.
44. Busico, V., Cipullo, R., and Talarico, G., *Macromolecules,* 1997, vol. 30, p. 4787.
45. Kleinschmidt, R., Reffke, M., and Fink, G., *Macromol. Rapid Commun.*, 1999, vol. 20, p. 284.
46. Brintzinger, H.H., Fischer, D., Muelhaupt, R., Rieger, R.B., and Waymouth, R.M., *Angew. Chem., Int. Ed. Engl.*, 1995, vol. 20, p. 1143.
47. Resconi, L., Cavallo, L., Fait, A., and Piemontesi, F., *Chem. Rev.,* 2000, vol. 100, p. 1253.
48. Guerra, G., Longo, P., Cavallo, L., Corradini, P., and Resconi, L., *J. Am. Chem. Soc.*, 1997, vol. 119, p. 4394.
49. Guerra, G., Cavallo, L., Moscadi, G., Vacatello, G., and Corradini, P., *J. Am. Chem. Soc.*, 1994, vol. 116, p. 2988.
50. Toto, M., Cavallo, L., Corradini, P., Moscardi, G., Resconi, L., and Guerra, G., *Macromolecules,* 1998, vol. 31, p. 3431.
51. Razavi, A., Peters, L., Nafpliotis, L., Vereecke, D., and Den Daw, K., *Macromol. Symp,* 1995, vol. 89, p. 345.
52. Razavi, A. and Thewalt, U., *J. Organomet. Chem.*, 2001, vol. 621, p. 267.
53. Razavi, A., Bellia, V., De Brauwer, Y., Hortmann, K., Lambrecht, M., Miserque, O., Peters, L., and van Belle, S., *Metalorganic Catalysts for Synthesis and Polymerization*, Kaminsky, W., Ed., Berlin: Springer, 1999, p. 236.
54. Yano, A., Kaneko, T., Sato, M., and Akimoto, A., *Macromol. Chem. Phys.*, 1999, vol. 200, p. 2127.
55. Eur. Pat. Appl. EP 155 050.
56. Int. Patent WO 98/54230; US Patent 6265505.
57. Int. Patent WO 98/54230.
58. Int. Patent WO 00/49029.
59. Eur. Patent EP 96111127.5.
60. Int. Patent WO 98/02469.
61. Eurt. Pat. Appl. 083188.
62. Int. Patent WO 00/49029; Eur. Pat. Appl. 169356.
63. Ferreira, M.L., Belelli, P.G., Juan, A., and Damini, D.E., *J. Mol. Catal. A: Chem.*, 1999, vol. 148, p. 127.
64. Ferreira, M.L., Belelli, P.G., and Damini, D.E., *Macromol. Chem. Phys.*, 2001, vol. 202, p. 495.
65. Borreli, M., Busico, V., Cipulla, R., and Rnoca, S., Budzelaar, P.H.M., *Macromolecules,* 2003, vol. 36, p. 8171.
66. Angermut, K., Fink, G., Jensen, V.R., and Kleinschmidt, R., *Chem. Rev.,* 2000, vol. 100, p. 1457.
67. Rappe, A.K., Skiff, W.M., and Casewitt, C.J., *Chem. Rev.*, 2000, vol. 100, p. 1391.
68. Alt, H.G., Jung, M., and Kehr, G., *J. Organomet. Chem.*, 1998, vol. 562, p. 153.
69. Drago, D., Pergosin, P.S., and Razavi, A., *Organometallics,* 2000, vol. 19, p. 1802.
70. Dash, A.K., Razavi, A., Mortreux, A., Lehmann, C., and Carpentier, J.F., *Organometallics,* 2002, vol. 21, p. 3238.
71. Kirilov, E., Toupet, L., Lehmann, C.W., Razavi, A., Kahlal, S., Saillard, J.Y., and Carpentier, J.F., *Organometallics,* 2003, vol. 22, p. 4038.
72. Kirilov, E., Toupet, L., Lehmann, C., Razavi, A., and Carpentier, J.F., *Organometallics,* 2003, vol. 22, p. 4467.
73. Kirilov, E., Lehmann, C., Razavi, A., and Carpentier, J.F., *Eur. J. Inorg. Chem.*, 2004, p. 943.
74. Kirilov, E., Lehmann, C., Razavi, A., and Carpentier, J.F., *Organometallics*, 2004, vol. 23, p. 2768.
75. Kirilov, E., Lehmann, C., Razavi, A., and Carpentier, J.F., *J. Am. Chem. Soc.*, 2004, vol. 126, p. 12240.
76. Bierwagen, E.P., Bercaw, J.E., and Goddard, W.A., *J. Am. Chem. Soc.*, 1994, vol. 116, p. 1481.
77. Chan, M.S.W. and Ziegler, T., *Organometallics,* 2000, vol. 19, p. 5182.
78. Zurek, E. and Ziegler, T., *Prog. Polym. Sci.*, 2004, vol. 29, p. 107.
79. Lansza, G., Fragala, I.L., and Marks, T.J., *J. Am. Chem. Soc.*, 1998, vol. 120, p. 8257.
80. Lansza, G., Fragala, I.L., and Marks, T.J., *J. Am. Chem. Soc.*, 2000, vol. 122, p. 12764.
81. Chen, M.C. and Marks, T.J., *J. Am. Chem. Soc.*, 2001, vol. 123, p. 11803.
82. Chen, M.C., Roberts, J.A.S., and Marks, T.J., *J. Am. Chem. Soc.*, 2004, vol. 126, p. 4605.
83. Zakharov, V.A., Zakharov, I.I., and Panchenko, V.N., *Organometallic Catalysts and Olefin Polymerization*, Blum, R.A., Follestad, R., Rytter, E., Tilset, M., and Ystenes, M., Eds., Berlin: Springer, 2001, p. 63.
84. Zakharov, V.A. and Zakharov, I.I., *Macromol. Theory Simul.*, 2001, vol. 10, p. 108.